

THEORETICAL MODEL FOR THE FLUIDELASTIC INSTABILITY OF TUBE BUNDLES

M. BENAOUICHA*, E. LONGATTE† AND F. BAJ‡

Laboratory for the Mechanics of Ageing Industrial Structures
LaMSID UMR EDF-CNRS-CEA 8193
1, avenue du Général de Gaulle
92141 Clamart CEDEX France
e-mail: *mustapha.benaouicha@ecole-navale.fr
†elisabeth.longatte@edf.fr
‡franck.baj@cea.fr

Key words: Fluidelastic instability, Tube bundle, Fluid-Structure Interaction

Abstract. *In this paper, a phase lag model is proposed in order to predict the fluid velocity threshold for a fluidelastic dynamic instability of square cylinder arrangement under cross flow. A theoretical formulation of a total damping, including the added damping in still fluid, the damping due to fluid flow and the damping derived from the phase shift between the fluid force and tube displacement, is given. A function of fluid and structure parameters, such as reduced velocity, pitch ratio, Scruton number, is thus obtained. It is shown that this function, taken as function of the reduced velocity variable, vanishes at the critical reduced velocity from which the fluidelastic dynamic instability of the tube occurs. Obviously, the value of the critical velocity is depending on other fluid-structure parameters. The obtained results are compared to experimental ones and those obtained from other theoretical models.*

1 INTRODUCTION

Fluidelastic instability is the most important of several flow-induced vibration excitation mechanisms that could cause excessive vibration in heat exchanger cylinder arrangements. Experience shows that most of heat exchanger tube vibration problems are related to fluidelastic instability [7, 13, 9, 10]. Indeed, in presence of high flow confinement, the thin cylinders could be subjected to strong vibrations, which may lead to instability development and therefore to a risk of break or collision. To prevent such problems, it is important to make a detailed analysis of flow-induced vibrations during design.

Several authors have addressed the problem of fluidelastic instability in cylinder arrangements. Experimental [7, 13, 8, 16] and theoretical approaches [9, 10, 19] have been in-

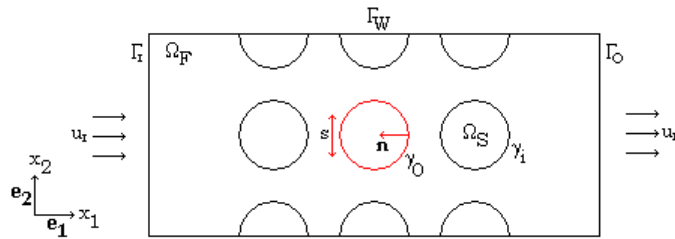


Figure 1: Square cylinder arrangement.

investigated. In order to understand the physics of the instability mechanisms and prevent them, many important theoretical models (see the review of [15]) and experimental results (see the review of [11]) have been produced. However, the contribution of various geometrical and fluid-structure parameters involved in the mechanism of fluidelastic instability remains elusive.

Other authors have tried to separate the phenomena to better understanding the mechanism of fluidelastic instability. The potential flow approximation was therefore used [1, 12, 3]. Unfortunately, it seems that inviscid flow theory is inadequate for stability analyses of cylinder arrays in cross flow [15, 2].

The purpose of this article is to improve the potential flow model by including a damping model which can make a good prediction of the velocity threshold for fluidelastic instability of a normal square tube bundle in cross flow. The model must be with sufficient accuracy, easy to implement and not expensive in computation time. Three damping terms are then included: (1) still fluid viscous damping, (2) fluid velocity-depending term and (3) a phase lag model in order to taking into account of the phase shift between the fluid force and tube displacement. The results are discussed and analyzed.

The obtained results are encouraging at this stage, comparing to available data from experiments and existing models. Fluid-structure interaction and flow-induced vibration in square cylinder arrangement under cross flow are investigated. In addition, the influence of key physical parameters on fluid-solid dynamics interaction is quantified.

2 COUPLED PROBLEM FORMULATION

2.1 Irrotational fluid flow

Let us consider a square arrangement cylinders immersed in a Newtonian, incompressible and irrotational ($\text{curl } u = 0$) fluid flow (FIGURE 1). Then there exist a scalar function $\Phi(x, t)$ so that the fluid velocity u is written as,

$$u = \nabla \Phi. \quad (1)$$

By using the fluid incompressibility condition and slip boundary conditions, the equation of Φ can be written as [6],

$$\left\{ \begin{array}{ll} \Delta\Phi = 0 & \text{on } \Omega_F \quad (a), \\ \nabla\Phi \cdot \mathbf{n} = -u_I & \text{on } \Gamma_I \quad (b), \\ \nabla\Phi \cdot \mathbf{n} = u_I & \text{on } \Gamma_O \quad (c), \\ \nabla\Phi \cdot \mathbf{n} = \dot{s} n_2 & \text{on } \gamma_0 \quad (d), \\ \nabla\Phi \cdot \mathbf{n} = 0 & \text{on } \Gamma_W \cup \gamma_{i,i \neq 0} \quad (e). \end{array} \right. \quad (2)$$

The fluid domain is denoted by Ω_F while Ω_S refers to the domain occupied by the tubes. In this study, only the middle tube is in a free transverse displacements, with a velocity \dot{s} , whereas the other tubes remain immobile. Let us denote by γ_0 the interface between Ω_F and the mobile cylinder and by $\gamma_{i,i \neq 0}$ the immobile cylinders. Γ_I stands for the inlet section, Γ_O the outlet section of the flow and Γ_W the wall (fixed boundary). $\mathbf{n} = (n_1, n_2)^T$ denotes the unit normal vector at $\partial\Omega_F = \Gamma_I \cup \Gamma_O \cup \Gamma_W \cup \gamma_i$ pointing out of Ω_F . The flow is taken perpendicular to the tubes with a velocity field u_I at the inlet Γ_I and outlet Γ_O .

2.2 Tube dynamics equations

The tube dynamics in the potential flow is governed by the following dimensionless second order differential equation :

$$\left\{ \begin{array}{l} \mathcal{M} \ddot{s}^* + \mathcal{D} \dot{s}^* + \mathcal{K} s^* = 0, \\ s^*(0) = s_0^*, \\ \dot{s}^*(0) = \dot{s}_0^*, \end{array} \right. \quad (3)$$

where $\mathcal{M} = (m_0 + m_a)/\rho d^2$ is the total mass ratio, \mathcal{D} the total tube damping and \mathcal{K} the total tube stiffness, including hydrodynamic quantities. m_0 , m_a and ρ represent respectively the tube mass, added mass and fluid mass density. $s^* = s/d$, $\dot{s}^* = \dot{s}/f_0 d$ and $\ddot{s}^* = \ddot{s}/f_0^2 d$ are the dimensionless tube displacement, velocity and acceleration. d represents the tube diameter and f_0 the natural tube frequency in air.

The added mass and stiffness are computed from potential flow, by considering the fluid force acting on the tube,

$$F = \int_{\gamma_0} P n_2 d\gamma_0, \quad (4)$$

where,

$$P = -\rho \left(\frac{\partial\Phi}{\partial t} + \frac{1}{2} |\nabla\Phi|^2 \right) + C(t), \quad (5)$$

is the pressure field in the fluid (Bernoulli formula) and $C(t)$ a constant that can be taken null.

The hydrodynamic damping resulting from irrotational flow is unfortunately inadequate for dynamic fluidelastic stability analysis of cylinder arrays in cross flow [15, 1]. A theoretical model for the total damping \mathcal{D} is needed to perform this analysis.

3 DAMPING MODEL

Three damping terms are included in total tube damping term \mathcal{D} . Still fluid viscous damping, flow-depending term and a phase lag model in order to taking into account of the phase shift between the fluid force and tube displacement.

3.1 Viscous damping

The still fluid damping gives rise, in non-dimensional case, to effective Scruton number,

$$Sc = 2 \pi \xi \mathcal{M}, \quad (6)$$

where ξ is the damping ratio in still fluid and $\mathcal{M} = \alpha_0 + \alpha_a$ the total dimensionless mass of the tube, derived from potential flow model [3], including the dimensionless added mass $\alpha_a = m_a/\rho d^2$. They can be analytically estimated by using the following formulas, developed by Chen et al. [5],

$$\alpha_a \approx \frac{\pi}{4} \frac{1 + \tau^2}{1 - \tau^2} + \sqrt{\frac{\pi}{St}}, \quad (7)$$

and

$$\xi \approx \frac{1}{f^* \mathcal{M}} \left[\alpha_0 \xi_0 + \frac{1}{2} \pi^{1/2} St^{-1/2} \beta_0 \right]. \quad (8)$$

The Scruton number is then given as,

$$Sc \approx \frac{1}{f^*} [Sc_0 + \pi^{3/2} St^{-1/2} \beta_0], \quad (9)$$

where $f^* = f/f_0$ is the dimensionless tube frequency in still fluid. It can be analytically estimated by using the following formula [4],

$$f^* = \frac{f}{f_0} = \sqrt{\frac{\alpha_0}{\mathcal{M}}}. \quad (10)$$

The Scruton number Sc_0 [18] being based on the structural damping ratio in air ξ_0 and fluid-structure mass ratio $\alpha_0 = m_0/\rho d^2$. The Stokes number is defined as,

$$St = f_0 d^2/\nu, \quad (11)$$

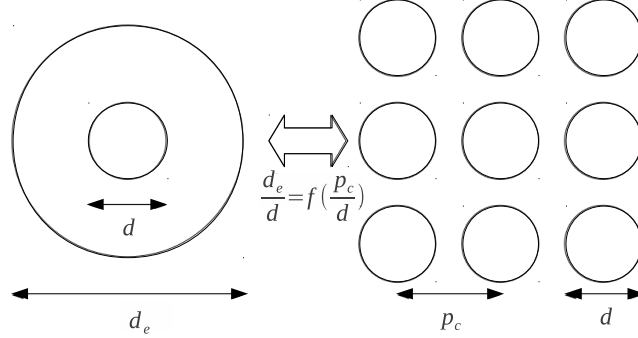


Figure 2: Rogers' equivalent confinement method

where ν is the kinematic viscosity coefficient, and β_0 is given by [5],

$$\beta_0 = \frac{1 + \tau^3}{(1 - \tau^2)^2}, \quad (12)$$

where τ , defined as [14],

$$\tau^{-1} = (1.07 + 0.56 p_r) p_r, \quad (13)$$

is the confinement parameter $\tau = d/d_e$ according to Rogers' method [17], which gives an equivalent confinement term for a tube bundle configuration in function of the confinement ratio of a cylinder in an annulus domain with external diameter d_e (Figure 2).

3.2 Flow-dependent damping

A dimensionless flow velocity-dependent fluid damping term as derived by [4] is also included, namely

$$\mathcal{D}_F(u_r) = (p_r - 1) u_r h, \quad (14)$$

or equivalently,

$$\mathcal{D}_F(u_{pr}) = \frac{(p_r - 1)^2}{p_r} u_{pr} h, \quad (15)$$

where $u_r = u_I/f_0 d$ is the fluid reduced velocity and u_{pr} defined as,

$$u_{pr} = \frac{u_p}{f_0 d}, \quad (16)$$

is the reduced pitch velocity. u_p being the pitch velocity, given by,

$$u_p = \frac{u_I}{1 - p_r^{-1}}, \quad (17)$$

$h = h(p_r)$ is a loss coefficient, function of a pitch ratio p_r . The experimental values of h versus pitch ratio [10] are fitted by using the following 4th order polynomial regression model for $1.2 \leq p_r \leq 2$ (Figure 3),

$$h_{pr} = a_0 + a_1 p_r + a_2 p_r^2 + a_3 p_r^3 + a_4 p_r^4, \quad (18)$$

where the coefficients

$$(a_i)_{i=0,\dots,4} = (52.39, -119.74, 103.38, -39.72, 5.72)$$

are obtained by the least square method,

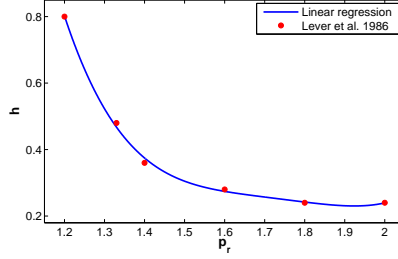


Figure 3: Loss coefficient.

The effective non-dimensional damping is then given as,

$$\mathcal{D} = 2Sc + \mathcal{D}_F + \mathcal{D}_\phi + \mathcal{C}, \quad (19)$$

where \mathcal{D}_ϕ is the damping derived from the phase angle ϕ between the fluid force and tube displacement [9, 10].

The essence of the present work is to give a simple theoretical model of \mathcal{D}_ϕ who can predict the critical velocity before dynamic instability occurrence.

3.3 Phase lag model

Let us consider a simple harmonic motion of the moving tube, given in dimensionless form, by the following equation,

$$s^* = s_0^* \cos(\omega^* t^*). \quad (20)$$

As the damping ratio ξ in potential flow is very small, the tube motion described by the equation (20) is the approximate solution of equation (3). $\omega^* = \omega/f_0$ being the dimensionless angular frequency in potential flow.

By considering the previous damping terms, the tube dynamics equation (3) can then be written as,

$$\begin{cases} \mathcal{M} \ddot{s}^* + (2Sc + (p_r - 1) h u_r + \mathcal{C}) \dot{s}^* + \mathcal{K} s^* = \mathcal{F}_\phi^*, \\ s^*(0) = s_0^*, \\ \dot{s}^*(0) = \dot{s}_0^*. \end{cases} \quad (21)$$

In the right side of the equation, the dimensionless hydrodynamic load \mathcal{F}_ϕ^* is introduced. It represents the part of the fluid load which is in out of phase ϕ with the tube displacement. In this study, it is assumed that the phase shift ϕ is space dependent and varies linearly from the immobile cylinder, at $x = -p_r$ ($\phi(-p_r) = 0$), to the moving cylinder, at $x = 0$ ($\phi(0) = \phi_0 \neq 0$). Figure (4) illustrates this assumption.

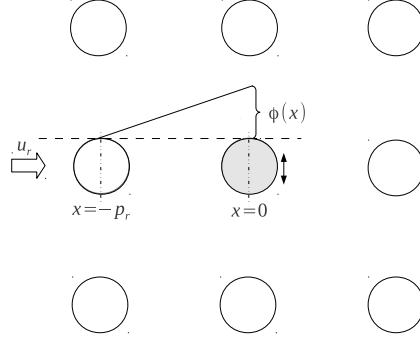


Figure 4: Linear dimensionless space variation of the force-displacement phase shift.

This means that the fluid force acting on the immobile cylinder, located upstream of the moving cylinder ($x = -p_r$), is in phase with the displacement of the tube ($\phi = 0$). While the phase shift is maximum ($\phi = \phi_0$) at the moving cylinder location ($x = 0$). For $-p_r \leq x \leq 0$, the phase variation is linear and given by,

$$\phi(x) = \left(\frac{x}{p_r} + 1\right)\phi_0. \quad (22)$$

The dimensionless fluid force at a point located between the mobile cylinder ($x = 0$) and the immobile one, upstream of the moving tube ($x = -p_r$), is then given as,

$$\begin{aligned} F_\phi^*(x) &= F_0^* \cos(\omega^* t^* + \phi(x)) = F_0^* \cos\left(\omega^* t^* + \left(\frac{x}{p_r} + 1\right)\phi_0\right) \\ &= \frac{F_0^*}{s_0^*} \left[s^* \cos\left(\left(\frac{x}{p_r} + 1\right)\phi_0\right) + \frac{\dot{s}^*}{\omega^*} \sin\left(\left(\frac{x}{p_r} + 1\right)\phi_0\right) \right], \end{aligned} \quad (23)$$

where F_0^* is the dimensionless magnitude of the fluid pressure.

We assume that the fluid force acting on the moving cylinder, is dependent only on the flow upstream the cylinder, until the immobile tube. To take into account this dependency, the sum over the interval $[-p_r, 0]$ of the force $F_\phi^*(x)$ is considered. The hydrodynamic force \mathcal{F}_ϕ^* (eq. 21) is then given as,

$$\begin{aligned} \mathcal{F}_\phi^* &= \int_{-p_r}^0 F_\phi^*(x) dx \\ &= \frac{p_r F_0^*}{\phi_0 s_0^*} \left[\sin(\phi_0) s^* + \frac{1}{\omega^*} (1 - \cos(\phi_0)) \dot{s}^* \right], \end{aligned} \quad (24)$$

As the interest of the model is to predict the dynamic instability threshold of the moving tube, only the damping part of \mathcal{F}_ϕ^* is then taken into account. The model of the total hydrodynamic damping \mathcal{D} (eq. 19), is then given as,

$$\mathcal{D} = 2Sc + (p_r - 1) h u_r + \mathcal{C} - \frac{p_r}{\phi_0 s_0^* \omega^*} (1 - \cos(\phi_0)) F_0^*, \quad (25)$$

where the damping due to the phase shift between the tube displacement and the fluid load, is given as a following model,

$$\mathcal{D}_\phi = -\frac{p_r}{\phi_0 s_0^* \omega^*} (1 - \cos(\phi_0)) F_0^*. \quad (26)$$

The values of ϕ_0 and F_0^* must be estimated.

Estimation of ϕ_0 The non-dimensional time relevant to the transient behaviour of an incompressible flow with finite fluid inertia can be shown to be [9, 20],

$$t^* = \frac{u_p}{p_c} t. \quad (27)$$

Thus the real time lag between the movement of the cylinder and the resultant movement of the streamline is measured in units time constant [9],

$$\tilde{t} = \frac{p_c}{u_p}. \quad (28)$$

In this study, the phase lag ϕ_0 between the fluid force and the cylinder displacement is estimated as,

$$\phi_0 = \omega \tilde{t} = \frac{\omega p_c}{u_p} = \frac{\omega^* p_r}{u_{pr}}, \quad (29)$$

or equivalently as,

$$\phi_0 = \frac{\omega^* (p_r - 1)}{u_r}. \quad (30)$$

Estimation of F_0^* As a first approximation, let us consider a stream tube bounded at each side by a streamline, assumed tangent to two adjacent cylinders (dash lines), as shown in figure (5).

The length of the stream tube being the center to center distance p_c and its width is $p_c - d$. The inlet flow velocity in the stream tube is the pitch velocity u_p . The gray cylinder being mobile, it is assumed that the fluid pressure F_0^* is proportional to the tube displacement magnitude s_0^* . It is given in dimensional form as,

$$F_0 = f_0^2 m_0 F_0^* = \frac{1}{2} \rho u_p^2 \frac{s_0}{d}, \quad (31)$$

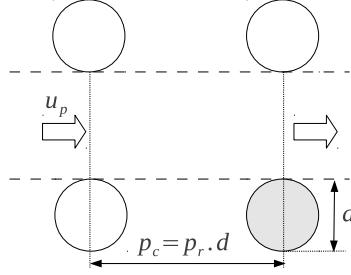


Figure 5: Stream tube in normal square cylinder arrangement.

The dimensionless magnitude of the fluid pressure is then given, as a function of a pitch reduced velocity, as,

$$F_0^* = \frac{s_0^*}{2\alpha_0} u_{pr}^2, \quad (32)$$

or equivalently, as a function of a reduced velocity, as,

$$F_0^* = \frac{s_0^*}{2\alpha_0(1-p_r^{-1})^2} u_r^2. \quad (33)$$

The following phase lag model of the damping term \mathcal{D}_ϕ , given in equation (26), is then derived by considering the equations (29) and (32),

$$\mathcal{D}_\phi(u_{pr}) = -\frac{1}{8\pi^2 f^{*2} \alpha_0} \left(1 - \cos\left(\frac{2\pi f^* p_r}{u_{pr}}\right) \right) u_{pr}^3, \quad (34)$$

or equivalently, by considering the equations (30) and (33),

$$\mathcal{D}_\phi(u_r) = -\frac{1}{8\pi^2 f^{*2} \alpha_0 (1-p_r^{-1})^3} \left(1 - \cos\left(\frac{2\pi f^* (p_r - 1)}{u_r}\right) \right) u_r^3, \quad (35)$$

where f^* is the non-dimensional natural tube frequency in still fluid, obtained from potential flow model.

The total hydrodynamic damping is then given as a function of the variable u_{pr} . It can be expressed as a fluid-structure parameters-depending function as,

$$\mathcal{D} = \mathcal{H}_{\mathcal{S}_c, f_0, f, p_r, \alpha_0}(u_{pr}), \quad (36)$$

or equivalently as a function of the variable u_r ,

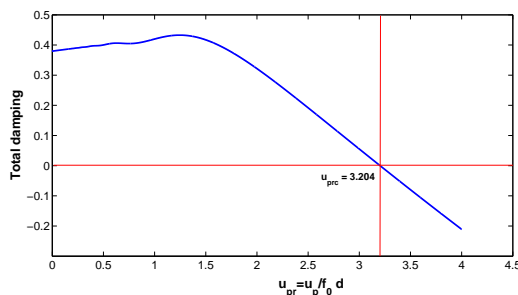
$$\mathcal{D} = \tilde{\mathcal{H}}_{\mathcal{S}_c, f_0, f, p_r, \alpha_0}(u_r) \quad (37)$$

The function \mathcal{H} is evaluated for different values of the fluid-structure parameters given in table (1). They represent an experimental data given in [13]. m being the total mass, including the hydrodynamic mass.

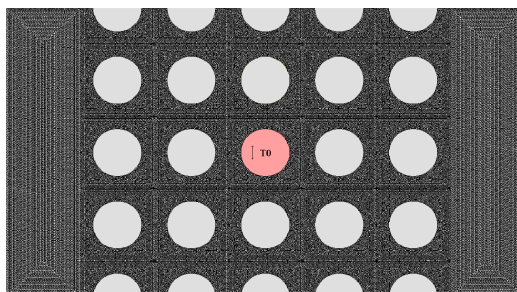
Case n°	p_r	d (mm)	m_0 (kg/m)	f_0 (Hz)	ξ_0 (%)	m (kg/m)	f (Hz)	Sc	$u_{pc}/f_0 d$
1	1.42	19.05	0.72	15.2	0.64	1.1	12.3	1.89E-1	2.56
2	1.42	19.05	0.72	25	0.61	1.1	20.2	2.78E-1	3.77
3	1.42	19.05	0.72	30	0.74	1.1	24.3	2.29E-1	4.15
4	1.5	25.4	0.607	25.5	0.22	1.257	16.9	1.07E-1	2.45
5	1.33	25.4	0.607	24.6	0.92	1.29	16.2	3.39E-1	2.09

Table 1: Considered cases [13]

The figure (6) shows the behaviour of the function \mathcal{H} for the fluid-structure parameters corresponding to the case 1 of table (1). First, the function is positive and increasing until it reaches its maximum. Then the function decreases to zero and becomes negative. The function has a unique root which corresponds to the value of the reduced pitch velocity u_{pr} , for which the total damping \mathcal{D} is zero and from which it becomes negative. This is the critical reduced pitch velocity u_{prc} before the tube dynamic instability occurrence. The behaviour of the function \mathcal{H} is the same for all other cases of table (1).


Figure 6: Effective damping versus pitch reduced velocity.

4 NUMERICAL RESULTS


Figure 7: Computational domain.

Consider a bundle of 25 tubes in normal square arrangement, immersed in a uniform fluid flow of mass density $\rho = 1000 \text{ kg/m}^3$ and kinematic viscosity coefficient $\nu = 10^{-6} \text{ m}^2/\text{s}$. The middle tube T_0 is in transverse motion, whereas the others are immobile (Figure 7). The problem (2) is solved by using the finite elements code CASTEM, to compute the tube's added mass m_a and natural frequency f in still fluid.

4.1 Validation of the model

The figure (8) shows the critical reduced pitch velocities obtained from the proposed model (equation 34) for various Scruton numbers corresponding to the cases given in table (1). A comparison to experimental results given by [13], Connors model [7], with fluidelastic instability constants $K = 3$ and $b = 0.5$, and Gorman model [8], with $K = 3.3$ and $b = 0.5$, is performed.

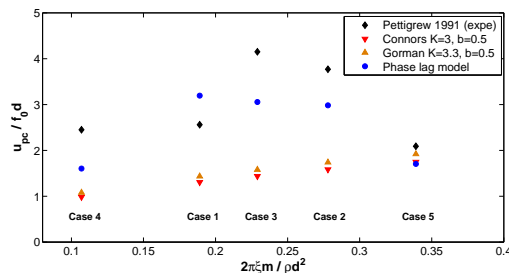


Figure 8: Comparison between theoretical models and experimental results.

The results obtained from the phase lag model (equation 34) are close to the experimental results, with deviations varying from 18.47% (for the case 5) to 34.5% (for the case 4). It is shown that the predictions obtained by the phase lag model are more accurate than those obtained by Connors and Gorman models, with the used fluidelastic instability constants. The results given by the phase lag model are encouraging at this stage but need to be validated further by considering more cases.

The results presented in the figure (8) are obtained by using experimental values of fluid-structure parameters given in [13]. The same parameters can be obtained by solving the coupled problem in potential flow (equations 2 and 3).

The figures (9, 10 and 11) show respectively the total tube mass, tube frequency in still fluid and total Scruton number for the considered cases (Table 1). For each case, the experimental and potential flow results are presented. It should be noted that the potential flow model allows, in most of the cases, to compute with a good accuracy the fluid-structure parameters. For the total mass, the deviations vary from 1% (for the three

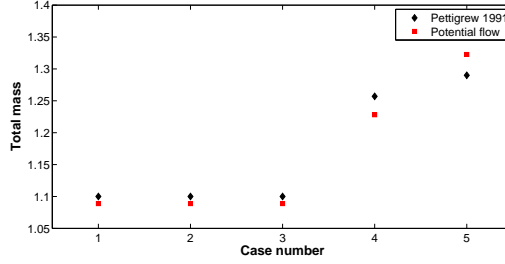


Figure 9: Total tube mass. Potential flow and experimental results.

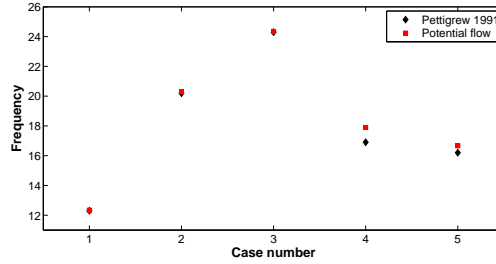


Figure 10: Tube frequency. Potential flow and experimental results.

first cases) to 2.56% (for the fifth case). For the natural frequency, the deviations vary from 0.32% (for the first case) to 5.86% (for the fourth case). For the total Scruton number, the deviations vary from 4.67% (for the fourth case) to 29.28% (for the second case) and 46.28% (for the fifth case).

The phase lag model (equation 34) can be used to predict the critical velocities, before dynamic tube instability occurrence, by considering the fluid-structure parameters derived from potential flow model or those obtained from experimental data. The figure (12) shows the comparison between the results obtained by the model in these two cases. They are also compared to experimental results given by [13].

It is shown that the results remain consistent when the experimental or potential flow values of the parameters are considered by the model. It should be noted that the deviation between the predicted critical velocities by the phase lag model is higher in the case 5 (Table 1). This is probably due to the bad estimation of the Scruton number in this case (Figure 11).

4.2 Dynamic instability analysis of the tube

The dynamic stability of the mobile tube in the case 1 (Table 1) is analysed by using the potential flow model enhanced by the phase lag model (equation 34). The critical reduced pitch velocity obtained in this case is $u_{prc} = 3.194$. It corresponds to the critical reduced velocity $u_{rc} = (1 - p_r^{-1}) u_{prc} = 0.9447$ (eq. 17). The displacement of the tube is

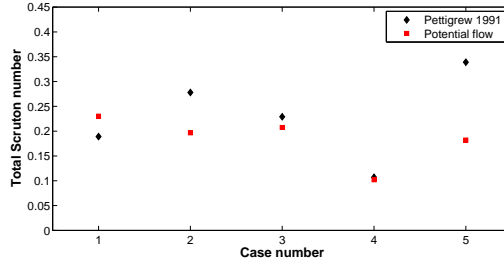


Figure 11: Total Scruton number. Potential flow and experimental results.

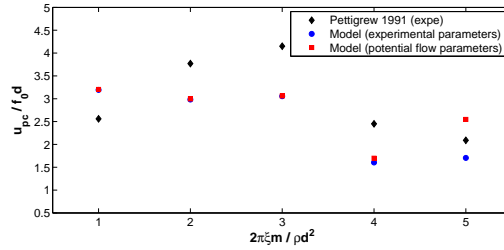


Figure 12: Critical reduced pitch velocity. Potential flow and experimental results.

computed for three reduced velocity values : $u_r = u_{rc}$, $u_r = 0.8 < u_{rc}$ and $u_r = 1 > u_{rc}$. The results are presented in figure (13). As expected, it is shown that for $u_r = u_{rc}$ the amplitudes of tube oscillations remain constant in time because of a zero total damping. The tube is then marginally stable. For $u_r = 0.8$ less than u_{rc} , the total damping is positive and the amplitudes of tube oscillations decreases. The tube is then stable. For $u_r = 1$ greater than u_{rc} , the total damping is negative and the amplitudes of the tube oscillations increases. These conclusions are in agreement with the phase trajectories presented in figure (14).

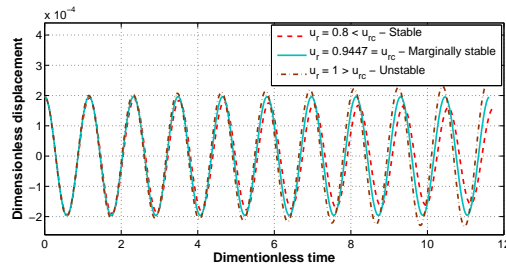


Figure 13: Displacement of the tube in case 1 for $u_r = u_{rc}$, $u_r < u_{rc}$ and $u_r > u_{rc}$.

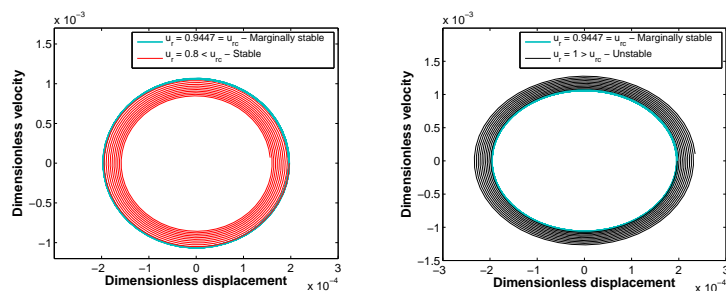


Figure 14: Phase trajectories of a tube in case 1.

5 CONCLUSION

A simple model is proposed to analyse a fluidelastic stability of square cylinder arrangement in cross flow. It is based on a potential flow model enhanced by a model describing the phase difference between the fluid force and tube displacement. The viscous and fluid velocity-dependent damping terms are also taken into account by the model. The phase lag model gives rise to a parameters-depending function of a variable u_r (reduced velocity). The parameters being the fluid-structure parameters such as mass-damping ratio, pitch ratio, frequency,... It is shown that the function has a unique root which corresponds to the critical reduced velocity before dynamic instability occurrence. The model is tested for several cases for which experimental results are available. The results are discussed and compared to reference data.

It is found that the phase lag model gives a good enough prediction of the reduced velocity threshold for the fluidelastic dynamic instability of normal square tube bundle in cross flow. The obtained results are close to existing results from experiments or other classical models. A single flexible tube behaviour, in transverse small amplitude motion, is then analysed. As expected, the tube is marginally stable, with constant amplitude, for a flow velocity equal to the predicted critical velocity. It becomes stable, with decreasing amplitude, for a fluid velocity less than the critical velocity. For a fluid velocity greater than the critical velocity, the fluidelastic dynamic instability occurs. The amplitude of tube motion increases and the tube is going to be unstable.

The proposed theoretical phase lag model is easy to implement. The results are fast obtained and are encouraging at this stage, but need further validations.

REFERENCES

- [1] T.F. Balsa. Potential flow interactions in an array of cylinders in cross-flow. *Journal of Sound and Vibration*, 50(2):285–303, 1977.
- [2] M. Benaouicha, E. Longatte, and F. Baj. Fluidelastic stability of tube bundles in potential flow. In *ERCOFTAC international symposium "Unsteady separation in fluid-structure interaction"*. Mykonos, Greece, June 17-21 2013.

- [3] M. Benaouicha, E. Longatte, and F. Baj. Stability of cylinder arrangement in potential flow. In *ASME Pressure Vessels and Piping Division Conference. Paris, France*, July 14-18 2013.
- [4] R.D. Blevins. *Flow-Induced Vibration*. New-york: Van nostrand reinhold edition, 1977.
- [5] S.S. Chen, M.W. Wanbgsanss, and J.A. Jendrzejczyk. Added mass and damping of a vibration rod in confined viscous fluid. *Journal of Applied Mechanics, Transaction of ASME*, 43:325–329, 1976.
- [6] C. Conca, J. Planchard, B. Thomas, and M. Vanninathan. *Problèmes mathématiques en couplage fluide-structure. Applications aux faisceaux tubulaires*. Eyrolles edition, 1994.
- [7] H.J. Connors. Fluid-elastic vibration of tube arrays excited by non-uniform cross-flow. *Flow-Induced Vibration of Power Plant Components*, 41:93–107, 1980.
- [8] D.J. Gorman. Experimental development of design criteria to limit liquid cross-flow-induced vibration in nuclear reactor heat exchange equipment. *Journal of Nuclear Science and Engineering*, 61:324–336, 1976.
- [9] J.H. Lever and D.S. Weaver. On the stability of heat exchanger tube bundles, part i : Modified theoretical model. *Journal of Sound and Vibration*, 107(3):375–392, 1986.
- [10] J.H. Lever and D.S. Weaver. On the stability of heat exchanger tube bundles, part ii : Numerical results and comparison with experiments. *Journal of Sound and Vibration*, 107(3):393–410, 1986.
- [11] M.P. Paidoussis. Flow-induced vibrations in nuclear reactors and heat exchangers: Practical experiences and state of knowledge. In *Practical experiences with flow-induced vibrations (eds E. Naudascher & D. Rockwell)*, pages 1–81. Berlin : Springer-Verlag, 1980.
- [12] M.P. Paidoussis, D. Mavriplis, and S.J. Price. A potential-flow theory for the dynamics of cylinder arrays in cross-flow. *Journal of Fluid Mechanics*, 146:227–252, 1984.
- [13] M.J. Pettigrew and C.E. Taylor. Fluidelastic instability of heat axchanger tube bundles: review and design recommendations. *Journal of Pressure Vessel Technology*, 113:242–256, 1991.
- [14] M.J. Pettigrew, C.E. Taylor, and A. Yasuo. Vibration damping of heat exchanger tube bundles in two-phase flow. *Welding Research Concl*, Bulletin 389:1–41, 1994.
- [15] S.J. Price. A review of theoretical models for fluidelastic instability of cylinder arrays in cross-flow. *Journal of Fluids and Structures*, 9:463–518, 1995.
- [16] S.J. Price and P. Paidoussis. The flow-induced response of a single flexible cylinder in an in-line array of rigid cylinders. *Journal of Fluids and Structures*, 3:61–82, 1989.

- [17] R.J. Rogers, C.E Taylor, and M.J. Pettigrew. Fluid effects on multi-span heat-exchanger tube vibration. In *ASME Pressure Vessels and Piping Division Conference. San Antonio, Texas*, 1984.
- [18] C. Scruton. Wind-excited oscillations of tall stacks. *The Engineer*, pages 806–808, 1955.
- [19] H. Tanaka, K. Tanaka, and F. Shimizu. Fluidelastic analysis of tube bundle vibration in cross-flow. *Journal of Fluids and Structures*, 16(1):93–112, 2002.
- [20] F.M. White. *Fluid Mechanics*. New-york: Mcgraw-hill edition, 1979.